Gamma-ray Showers Observed at Ground Level in Coincidence With Downward Lightning Leaders

R.U. Abbasi[1], T.Abu-Zayyad [1], M. Allen [1], E. Barcikowski [1], J.W. Belz[1], D.R. Bergman[1],

S.A. Blake[1], M. Byrne[1], R. Cady[1], B.G. Cheon[4], J. Chiba[5], M. Chikawa[6], T. Fujii[7],

M. Fukushima[7,8], T. Goto[9], W. Hanlon[1], Y. Hayashi[9], N. Hayashida[10], K. Hibino[10],

K. Honda[11], D. Ikeda[7], N. Inoue[2], T. Ishii[11], H. Ito[12], D. Ivanov[1], S. Jeong[13], C.C.H. Jui[1],

K. Kadota[14], F. Kakimoto[3], O. Kalashev[15], K. Kasahara[16], H. Kawai[17], S. Kawakami[9],

K. Kawata[7], E. Kido[7], H.B. Kim[4], J.H. Kim[1], J.H. Kim[18], S.S. Kishigami[9], P.R. Krehbiel[19],

V. Kuzmin[15], Y.J. Kwon[20], J. Lan[1], R. LeVon[1], J.P. Lundquist[1], K. Machida[11], K. Martens[8],

T. Matsuda[21], T. Matsuyama[9], J.N. Matthews[1], M. Minamino[9], K. Mukai[11], I. Myers[1],

K. Nagasawa[2], S. Nagataki[12], R. Nakamura[27], T. Nakamura[22], T. Nonaka[7], S. Ogio[9],

M. Ohnishi[7], H. Ohoka[7], K. Oki[7], T. Okuda[23], M. Ono[24], R. Onogi[9], A. Oshima[25],

S. Ozawa[16], I.H. Park[13], M.S. Pshirkov[14,26], J. Remington[1], W. Rison[19], D. Rodeheffer[19],

D.C. Rodriguez[1], G. Rubtsov[15], D. Ryu[18], H. Sagawa[7], K. Saito[7], N. Sakaki[7], N. Sakurai[9],

T. Seki[27], K. Sekino[7], P.D. Shah[1], F. Shibata[11], T. Shibata[7], H. Shimodaira[7], B.K. Shin[9],

H.S. Shin[7], J.D. Smith[1], P. Sokolsky[1], R.W. Springer[1], B.T. Stokes[1], T.A. Stroman[1],

T. Suzawa[2], H. Takai[29], M. Takeda[7], R. Takeishi[7], A. Taketa[30], M. Takita[7], Y. Tameda[31],

H. Tanaka[9], K. Tanaka[32], M. Tanaka[21], R.J. Thomas[19], S.B. Thomas[1], G.B. Thomson[1],

P. Tinyakov[14,32], I. Tkachev[15], H. Tokuno[3], T. Tomida[27], S. Troitsky[15], Y. Tsunesada[9],

Y. Uchihori[34], S. Udo[10], F. Urban[33], G. Vasiloff[1], T. Wong[1], M. Yamamoto[27], R. Yamane[9],

H. Yamaoka[21], K. Yamazaki[30], J. Yang[7], K. Yashiro[5], Y. Yoneda[9], S. Yoshida[17], H. Yoshii[35],

Z. Zundel[1]

[1]High Energy Astrophysics Institute and Department of Physics and Astronomy, University of Utah, Salt Lake City, Utah,

USA

[2]The Graduate School of Science and Engineering, Saitama University, Saitama, Saitama, Japan

[3]Graduate School of Science and Engineering, Tokyo Institute of Technology, Meguro, Tokyo, Japan

[4]Department of Physics and The Research Institute of Natural Science, Hanyang University, Seongdong-gu, Seoul, Korea

[5]Department of Physics, Tokyo University of Science, Noda, Chiba, Japan

[6]Department of Physics, Kinki University, Higashi Osaka, Osaka, Japan

[7]Institute for Cosmic Ray Research, University of Tokyo, Kashiwa, Chiba, Japan

[8]Kavli Institute for the Physics and Mathematics of the Universe (WPI), Todai Institutes for Advanced Study, the University

of Tokyo, Kashiwa, Chiba, Japan

[9]Graduate School of Science, Osaka City University, Osaka, Osaka, Japan

[10]Faculty of Engineering, Kanagawa University, Yokohama, Kanagawa, Japan

[11]Interdisciplinary Graduate School of Medicine and Engineering, University of Yamanashi, Kofu, Yamanashi, Japan

[12]Astrophysical Big Bang Laboratory, RIKEN, Wako, Saitama, Japan

[13]Department of Physics, Sungkyunkwan University, Jang-an-gu, Suwon, Korea

[14]Department of Physics, Tokyo City University, Setagaya-ku, Tokyo, Japan

[15]National Nuclear Research University, Moscow Engineering Physics Institute, Moscow, Russia

[16]Advanced Research Institute for Science and Engineering, Waseda University, Shinjuku-ku, Tokyo, Japan

[17]Department of Physics, Chiba University, Chiba, Chiba, Japan

[18]Department of Physics, School of Natural Sciences, Ulsan National Institute of Science and Technology, UNIST-gil,

Ulsan, Korea

[19]Langmuir Laboratory for Atmospheric Research, New Mexico Institute of Mining and Technology, Socorro, New Mexico

87801, USA.

[20]Department of Physics, Yonsei University, Seodaemun-gu, Seoul, Korea

[21]Institute of Particle and Nuclear Studies, KEK, Tsukuba, Ibaraki, Japan

[22]Faculty of Science, Kochi University, Kochi, Kochi, Japan

[23]Department of Physical Sciences, Ritsumeikan University, Kusatsu, Shiga, Japan

[24]Department of Physics, Kyushu University, Fukuoka, Fukuoka, Japan

[25]Engineering Science Laboratory, Chubu University, Kasugai, Aichi, Japan

[26]Sternberg Astronomical Institute Moscow M.V.Lomonosov State University, Moscow, Russia

[27]Department of Computer Science and Engineering, Shinshu University, Nagano, Nagano, Japan

[28]Department of Physics and Astronomy, Rutgers University - The State University of New Jersey, Piscataway, New Jersey,

USA

[29]Brookhaven National Laboratory, Upton, New York, USA

[30]Earthquake Research Institute, University of Tokyo, Bunkyo-ku, Tokyo, Japan

[31]Department of Engineering Science, Faculty of Engineering, Osaka Electro-Communication University, Neyagawa,

Osaka, JAPAN

[32]Graduate School of Information Sciences, Hiroshima City University, Hiroshima, Hiroshima, Japan

[33]Service de Physique Théorique, Université Libre de Bruxelles, Brussels, Belgium

[34]National Institute of Radiological Science, Chiba, Chiba, Japan

[35]Department of Physics, Ehime University, Matsuyama, Ehime, Japan

Abstract

Bursts of energetic particle showers have been observed in coincidence with downward prop-agating negative leaders in lightning flashes by the Telescope Array Surface Detector (TASD). The TASD is a 700 square kilometer cosmic ray observatory located in western Utah. Light-ning position, time, and electric field information was collected by a lightning mapping array and slow antenna colocated with the TASD. The observed showers arrived in bursts lasting several hundred microseconds, and were associated with the initial stages of leaders at an al-titude of a few kilometers above ground level prior to cloud-to-ground lightning strikes. Sim-ulation studies indicate that the observed showers are consistent with originating in forward-beamed primary gamma rays, from a source altitude greater than one kilometer above the ground and distributed according to a relativistic runaway electron avalanche spectrum with energies greater than 100 keV. We conclude that the showers observed are compatible with downward terrestrial gamma ray flashes (TGFs), and provide new insights into the TGF phe-nomenon.

1 Introduction

Terrestrial gamma ray flashes (TGFs) are bursts of gamma rays initiated in the Earth's atmosphere, first reported in 1994 from the Burst and Transient Source Experiment (BATSE) on the Compton Gamma-Ray Observatory satellite [*Fishman et al.*, 1994; *Kouveliotou*, 1994]. Since then, a number of observations have shown that satellite-detected TGFs are produced by lightning flashes. In particular, the observations indicate that the TGFs are produced by relativistic runaway electron avalanches (RREAs) [*Dwyer and Smith*, 2005; *Dwyer*, 2008, 2012; *Dwyer et al.*, 2012b], within the first few milliseconds of upward intracloud (IC) flashes [*Stan-ley et al.*, 2006; *Shao et al.*, 2010; *Lu et al.*, 2010; *Cummer et al.*, 2011, 2015; *Lyu et al.*, 2016]. In normally-electrified storms, intracloud flashes occur between the main mid-level negative and the upper positive charge region. They typically begin with upward-developing negative breakdown (e.g. *Shao and Krehbiel* [1996] and *Behnke et al.* [2005]), thus their de-tection in overhead satellites.

Since their discovery, an important question has been whether TGFs can be detected at ground level. Four gamma-ray observations have been detected by ground experiments: two of the experiments have reported observations of gamma-rays after the return stroke, in-dicating that gamma rays seen on the ground may originate from a mechanism different from that of the previous TGF satellite events. *Dwyer et al.* [2012a] at the International Center for

Lightning Research and Testing (ICLRT) and *Tran et al.* [2015] at the Lightning Observatory in Gainesville (LOG) reported observing gamma-rays during the first stroke of a natural –CG flash, about 200 μs after the beginning of the upward return stroke. The other two, *Dwyer et al.* [2004] and *Hare et al.* [2016] at the ICLRT reported gamma-ray observations in association with upward positive leaders in rocket-triggered lightning. Both occurred several kilometers Above Ground Level (AGL).

The fact that satellite-detected TGFs appear to be produced during upward negative breakdown at the beginning of intracloud discharges suggests that TGFs should also be produced by the downward negative breakdown that occurs at the beginning of –CG flashes. In this paper we present the first observations that this indeed happens. In particular, we report detections of TGF-like particle showers detected by Telescope Array (TA) cosmic ray facility in western Utah. The detections were identified by correlating Telescope Array Surface Detector (TASD) events with lightning data from the National Lightning Detector Network (NLDN), a Lightning Mapping Array (LMA), and electrostatic field change (ΔE) measurements. From measurements obtained over a 2.5–year period between 2013 and 2016, a total of ten TGF bursts were identified for which 3-D LMA or ΔE lightning measurements were available. In each case the parent flash was a –CG discharge and the burst occurred within the first or second millisecond of the flash.

Previous ground–based x– and gamma–ray observations have primarily utilized NaI detectors, but with limited areal coverage. The TASD of the present study utilize large-area (3 m^2) plastic scintillators that are optimized for detecting high-energy charged particles produced in cosmic ray air showers. While lacking the ability to measure the energy of individual particles, the TASD response time is roughly ten times faster than that of NaI detectors. Moreover, the TASD covers an area hundreds of times larger than other ground-based detectors of lightning-associated events, making it the largest lightning detector to date. The addition of an LMA network and ΔE observations to the TASD has provided us with a unique suite of instruments for studying TGF phenomena.

2 Telescope Array, and Lightning Mapping Array, and Slow Antenna Detectors

2.1 The Telescope Array Surface Detector

The Telescope Array (TA) is located in the southwestern desert of the State of Utah, and was commissioned with the primary goal of detecting Ultra High Energy Cosmic Rays (UHECRs). It is composed of a 700 km^2 Surface Detector array (SD), overlooked by three

Fluorescence Detector (FD) sites [*Abu-Zayyad et al.*, 2013a] (See Fig. S1). The FD, which operates on clear moonless nights (approximately 10% duty cycle) provides a measurement of the longitudinal profile of the Extensive Air Shower (EAS) induced by the primary UHECR, as well as a calorimetric estimate of the EAS energy. The SD part of the detector, with 100% duty cycle, provides shower footprint information including core location, lateral density profile, and timing, which are used to reconstruct shower geometry and energy.

The TASD is currently comprised of 507 scintillator detectors on a 1.2 km square grid. Each detector unit consists of two 3 m^2 scintillator planes, each plane is 1.2 cm thick. The two planes are separated by a 1 mm thick steel plate, and are read out by individual photomultiplier tubes (PMTs) which are coupled to the scintillator via an array of wavelength-shifting fibers. The scintillator, fibers and photomultipliers are contained in a light-tight stainless steel box under an additional iron roof providing protection from extreme temperature variations [*Abu-Zayyad et al.*, 2013a] (See Fig. S1).

The output signals from the PMTs are digitized locally by a 12 bit Fast Analog-to-Digital Converter FADC with a 50 MHz sampling rate [*Nonaka et al.*, 2009]. Each detector unit also has a 1 m^2 solar panel, a stainless steel box placed under the solar panel housing the battery and the front-end electronics, and a 2.4 GHz wireless LAN modem communication antenna transmitting data to communication towers.

The Telescope Array Surface Detector (TASD) is designed to detect the charged components (primarily electrons, positrons, and muons) of the EAS. An event trigger is recorded when three adjacent SDs observe a signal greater than 3 Minimum Ionizing Particles (MIPs) within 8 μs. When a trigger occurs, the signals from all the SDs within $\pm$ 32 μs and amplitude greater than 0.3 MIP are also recorded. The typical SD trigger rate is less than one per hundred seconds (0.01 Hz). The trigger efficiency of UHECRs with zenith angle less than 45° and energy greater than 10 EeV is approximately 100%, with an aperture of 1,100 km^{2}sr [*Abu-Zayyad et al.*, 2013a].

After a trigger is established, the arrival timing and lateral distribution of the event is used to reconstruct the event's arrival direction and energy. While the TASD is designed to provide good timing information for high-energy charged particles produced in cosmic-ray induced EAS, measuring energy for individual particles is not possible. Rather, the energy of the EAS (and hence the primary cosmic ray) is estimated by counting the effective number of MIPs in the individual scintillator, as a function of the lateral distance from the shower core.
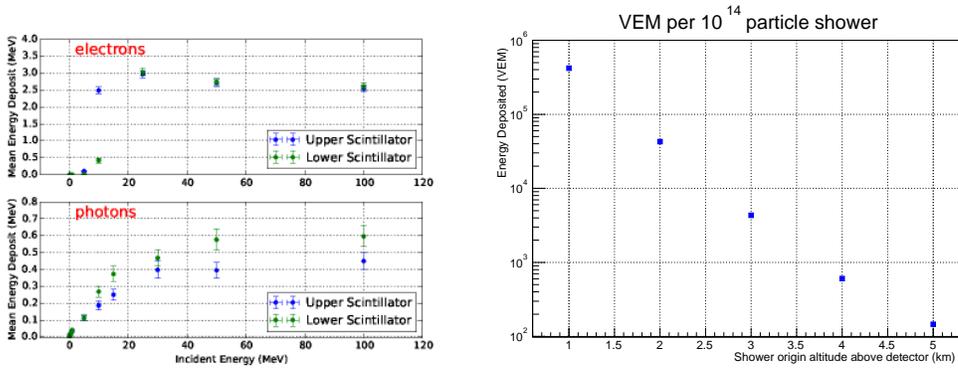
Figure 1. *Left:* Results of Geant4 simulation of mean TASD energy deposit for incident electrons and photons. *Right:* Energy deposit (VEM units) in a TASD scintillator in the path of a 10^{14}-photon RREA shower, as a function of shower altitude, with energy and angular distributions as described in the text.

To understand the response of the TASD to photons and low-energy electrons we performed a detailed Geant4 [*Agostinelli et al.*, 2003; *Allison et al.*, 2006] simulation of the individual scintillator response [*Ivanov*, 2012]. The detector steel and scintillators were included in the simulation, along with supporting structure, as was the earth under the detector which could contribute to signal via backscatter. Energy deposited in the upper and lower planes of scintillator is recorded as a function of incident particle energy for a large number of primary particles incident on the virtual scintillation detector. Mean energy deposit was recorded in the upper and lower scintillator as a function of incident particle energy as shown in Fig. 1. Electrons above 10 MeV (20 MeV) are expected to deposit the same energy as MIPs in the upper (lower) scintillator. High-energy photons on average will deposit about one fifth of the energy of a MIP, due to inefficient conversion via Compton scattering in the detector steel and scintillator.

2.2 The Lightning Mapping Array and Slow Antenna

The Lightning Mapping Array (LMA) was developed by the Langmuir Laboratory group at New Mexico Tech [*Rison et al.*, 1999; *Thomas et al.*, 2004]. The LMA produces detailed 3-D images of the VHF radiation produced by lightning inside storms. A nine-station network of sensors was deployed in 2013 over the 700 km^2 area covered by the TA detector. It detects the peak arrival time of impulsive radio emissions in a locally unused TV channel, in this case U.S. Channel 3 (60-66 MHz). In radio-quiet areas such as the south-

western Utah desert, the LMA detects VHF emissions over a wide (>70 dB) dynamic range, from ≤10 mW to more than 100 kW peak source power. Cell data modems connect each station into the internet, allowing decimated data to be processed in real time and posted on the web, and for monitoring station operation.

During 2014, a slow antenna (SA) recorded electric field changes of the lightning discharges. The SA was located in the center of the TASD and continuously recorded 10 kHz, 24-bit sampled data from a downward-looking flat plate sensor (e.g., *Krehbiel et al.* [1979]). The data were stored locally on 256 GB SD cards, and accurately measured electric field changes over the range of 10 mV/m to 10 kV/m with a decay time constant of 10 seconds.

3 Observations

Following *Okuda* [2016], we searched for candidate lightning events in the TASD dataset by identifying instances in which "bursts" of consecutive TASD triggers were recorded in 1 ms time intervals. Since the TASD mean trigger rate from cosmic ray event is less than 0.01 Hz, it is extremely unlikely that such bursts could be caused by the accidental coincidence of high-energy cosmic rays.

Figure 2 shows an example of a typical set of SD waveforms and the corresponding TASD footprint from a trigger burst event. As in the standard TASD analysis for cosmic rays, the integrated area under the photomultiplier waveform, relative to that expected for a single minimum-ionizing muon, gives the *Vertical Equivalent Muon* (VEM) count by which each SD trigger is characterized. One VEM corresponds to ≃ 2.05 MeV of energy deposited in the 1.2 cm thick scintillator. The footprint plot shows the VEM counts for each participating surface detector, with size proportional to the logarithm of the total energy deposited.

The waveforms recorded in the lightning-correlated bursts are different from those observed for cosmic rays as shown in Fig. S3. In a typical cosmic ray event, the photomultiplier waveforms for SDs near the core (center-of-energy deposit) of the event are characterized by a single sharply defined shower front followed by a tail consistent with the expected shower thickness for a log normal-like signal. The upper and lower scintillator waveforms are well-matched [*Abu-Zayyad et al.*, 2013b]. In contrast with this, the waveforms recorded during lightning bursts tend to show a slower rise and fall in the signal waveform. Also, the upper and lower scintillator waveforms are not well matched, due to inefficient conversion of photons in the scintillator detectors.
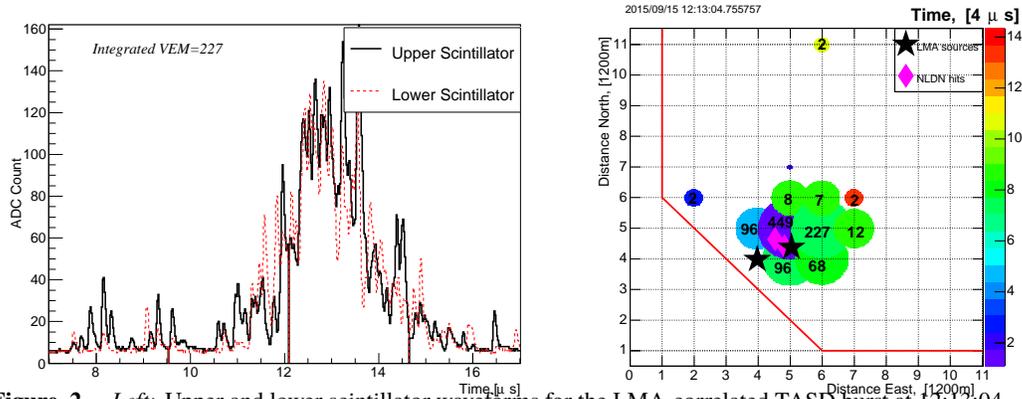
Figure 2. *Left:* Upper and lower scintillator waveforms for the LMA-correlated TASD burst at 12:13:04 on 15 Sept. 2015 (Fig. 3a). *Right:* Footprint of TASD triggers for the event, with the numbers indicating the Vertical Equivalent Muon (VEM) counts (see text), and the color indicating the relative arrival times. Initial LMA and NLDN events are indicated by stars and diamonds respectively. The red line indicates the southwestern boundary of the TASD array.

3.1 LMA-Correlated TASD Bursts

Due to being operated in a remote location with minimal maintenance and support, the LMA and slow antenna coverage was intermittent during the 3-year period between 2013 and 2016. However, three TASD bursts were observed in coincidence with LMA activity during this time. Figure 3 shows how the TASD trigger times were related to the LMA height-time and NLDN observations. In each case the triggers (dashed red lines) occurred at the very beginning of the flash (left panels). Flashes FL1 and FL2 occurred on 15 Sept 2015. LMA observations show they began as low-altitude intracloud discharges between mid-level negative charge at ≈ 5–6 km M.S.L. (upper level sources in panels a and c) and lower positive charge at ≈ 2.5–3.5 km M.S.L. (lowâĂŞaltitude sources) (Figs. S12 and S13, and [*Thomas et al.*, 2001]). Only toward the end of each flash, approximately 200 and 300 ms later, did the flashes produce strokes to ground.

To obtain a more complete picture of the temporal correlations, the zoomed-in panels (right side of Figure 3) show additional LMA sources having relaxed goodness-of-fit values (starred symbols). The altitudes of the these and the higher power sources often have significant error, due to being non-impulsive, VHF-noisy events. The timing and source powers of the events are reasonably well-determined, however, and show that several TASD triggers were associated with high power LMA events. The correlated NLDN observations had peak current values of between 9 and 22 kA (Figure 3b, d and Table S1).
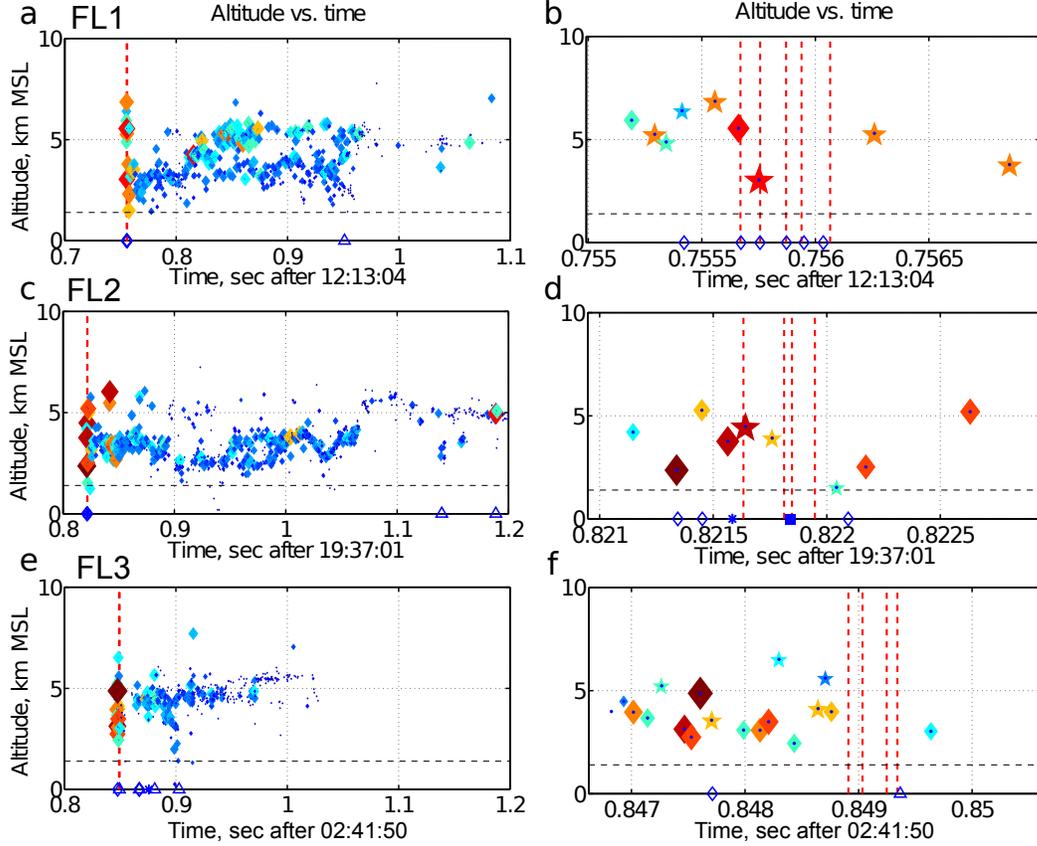
Figure 3. Observations of the LMA-correlated TASD bursts, showing altitude vs. time plots of the LMA sources (colored diamonds) and the TASD trigger times (red dashed lines). The left panels show the complete flashes and the right panels show zoomed-in views during the first 2–3 ms of each flash. The LMA sources are colored and sized by the log of their radiated power, and range from source powers of –20 dBW (10 mW; blue colors) up to +25 dBW (320 W; red colors). NLDN events are shown on the abscissa: $\diamond$ = –IC, $\triangle$ = –CG, $\blacksquare$ = +IC, $*$ = +CG. The mean altitude of the Telescope Array was ~1.4 km MSL (horizontal dashed line). In the zoomed-in plots, the altitude values are mostly in error due to relaxing the goodness of χ^2 criteria for source determination. Sources in the left panels have $\chi^2_\nu \leq 5$; starred sources in the right panels have χ^2_ν values between 5 and 500.

From the above we can safely conclude that the TASD-triggering showers for FL1 and FL2 originated somewhere between $\approx$ 3 and 5 km MSL ($\approx$ 1.5 and 3.5 km AGL). This occurred within the first ms of each flash as the initial negative breakdown descended into the lower positive charge region. The TASD triggers were centered below the initial LMA and NLDN sources (Figure 3 and S5), consistent with the triggering events being downwardly beamed and consistent with the RREA simulations of Figure 1.

Flash FL3 occurred on 10 May 2016. While the LMA sources in the leader stage were at an altitude comparable to those in FL2, the TASD triggers occurred later (approximately 2 ms) relative to the initial breakdown. The presence of a –94 kA NLDN ground stroke 2.6 ms after the initial breakdown suggests that this stepped leader was highly energetic, with an average propagation speed of 1.4×10^6 m/s, an order of magnitude faster than the speed of typical stepped leaders. From this, the first TASD trigger occurred when the leader was nominally $\approx$ 640 m above ground, and the last $\approx$ 40 m (25 μs) above ground. The vertical equivalent muon (VEM) count in the nearest surface detector was at least 22,000 (45 GeV energy deposition) for the last TASD trigger. This compares to VEM values of a few tens to a few hundreds for other events of this study (Table S1), and is likely due to the lower source altitude. Still in need of resolution within this interpretation however is the fact that the earlier triggers of FL3 had similar footprints on the ground (Figure S5) as the higher altitude events of FL1 and FL2.

The TGF-producing flash reported by *Dwyer et al.* [2012b] (their Figure 1) produced a similarly strong radiation burst in the final stages of the flashâĂŹs initial leader. Their prestroke leader activity was determined to be produced by *x*- rather than gamma-rays. However that is unlikely to be the case here: The absorption length of photons with energy less than 100 keV would be of order 10 meters, far too short to produce the minimum several-square kilometer footprint required by all TASD triggers.

3.2 Slow Antenna-Correlated TASD Bursts

Slow electric field change observations were available only during the 2014 storm season. Seven TASD trigger bursts were correlated with the observations. The flashes occurred on three different days in 2014, during times when LMA data was not available. Nevertheless, the slow antenna waveforms are readily understood [*Krehbiel et al.*, 1979]. As seen for flashes FL1 and FL2 of the LMA correlations, the TASD trigger bursts occurred in the first millisecond of the flash for each of the seven events.

Two events (flashes FL4 and FL8), had normal–duration initial leaders (28 ms and 14 ms) and typical peak currents (–12.2 and –11.7 kA). Of the remaining five events, three had intermediate–duration initial leaders between 4 and 10 ms (FL7, FL9 and FL10; I_{pk} = –66.6, –16.1, –35.0 kA, respectively). The remaining two (FL5 and FL6) had fast, short–
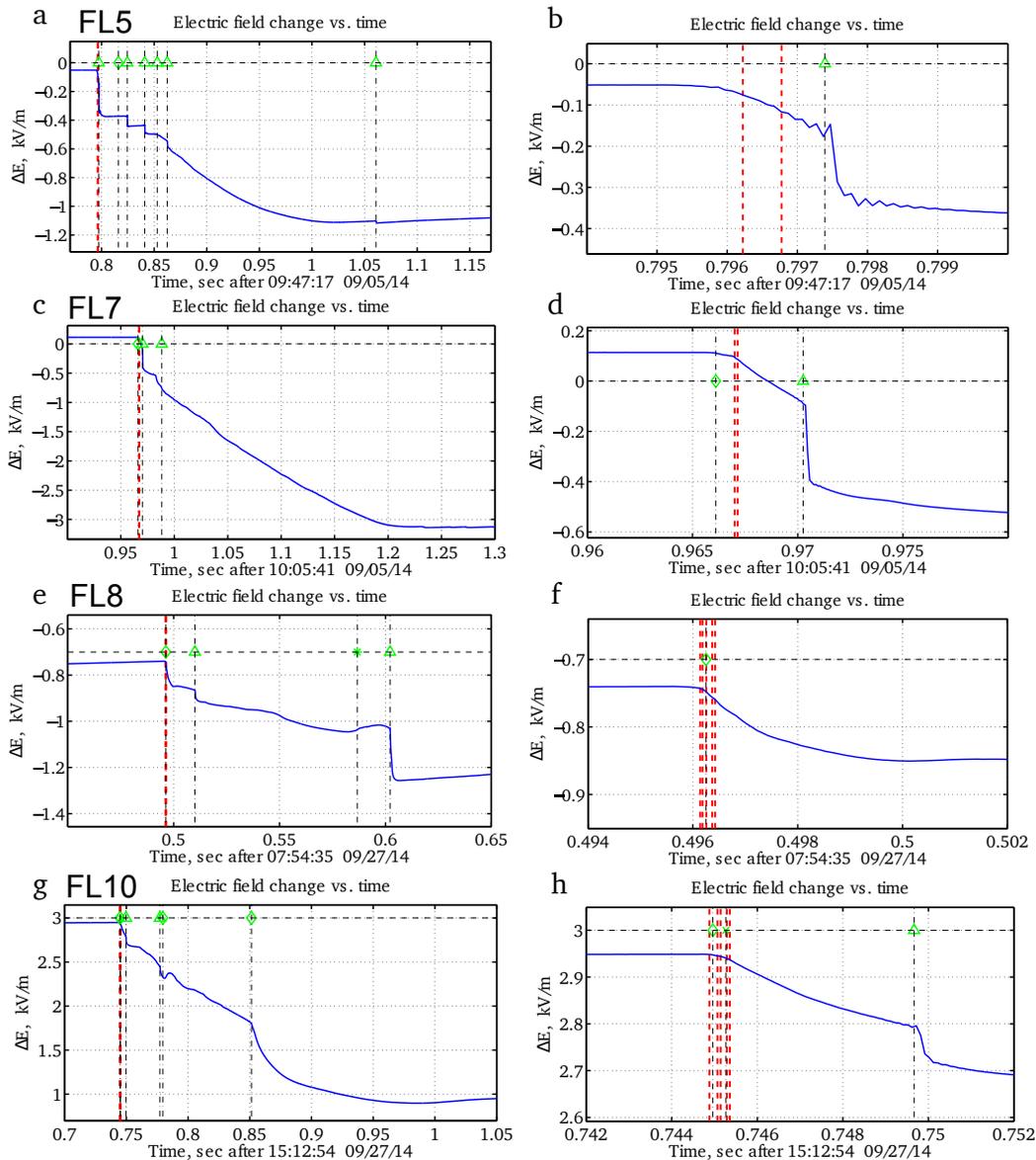
Figure 4. Electric field change versus time for four of the slow-antenna correlated trigger burst events (Flashes 5, 7, 8 and 10). The dashed lines and green symbols indicate the times and type of NLDN events (△, ◇, ✕, ✳ = –CG, –IC, +CG, +IC, respectively). The long negative field changes at the end of flashes are continuing current discharges to ground. The left side panels cover the entire burst, while the right side details a particular feature.

duration leaders (1.5–2.5 ms) and correspondingly strong return strokes (–140 kA and –101 kA peak). Thus the TASD trigger were not exclusively associated with energetic leaders.

The observations are illustrated in Figure 4, which shows correlation results for flashes 5, 7, 8 and 10 (the rest of flashes are shown in Fig. S4). The overall ΔE waveforms are characteristic of multiple-stroke negative cloud-to-ground discharges (left panels). Of interest here is the duration of the TASD bursts relative to the leader duration. As can be seen qualitatively from the plots, except for FL5, the burst durations are a relatively small fraction of the leader duration. The fractional durations for (FL7,FL8, and FL10) of Fig. 4 are $\simeq 3.4\%$, 2.1%, and 10%. Assuming for simplicity the leaders were nominally 5 km in length and propagated to ground at a constant speed, the above percentages indicate extents of 170 m, 100 m and 500 m for the burst periods. For comparison, the stepping lengths of upward negative breakdown at the beginning of intracloud flashes is $\simeq$ 500 m (*Rison et al.* [2016]). Because the stepping lengths will be shorter at the lower altitude (higher pressure), the above values are qualitatively consistent with the bursts being associated with the stepping of the initial breakdown of the flash. The fractional duration for FL5 is approximately 22%, the TASD triggers are probably indicative of separate events during the leader descent but are also perhaps the result of an extensive burst similar in duration to bursts reported by [*Dwyer et al.*, 2012a; *Tran et al.*, 2015; *Dwyer et al.*, 2004; *Hare et al.*, 2016].

A future, more detailed analysis of the TASD bursts will utilize timing information in the surface detectors to determine precisely the arrival directions of the lightning-correlated showers. The current TASD measurements show the activity to be temporally resolved into discrete few-microsecond sub-events (Fig. S9-S11) which last over a duration of a few hundred microseconds. Careful use of the TASD timing information will allow the origins of these sub-events to be resolved.

4 Discussion

In this paper we report observations of energetic particle showers produced during downward initial negative breakdown at the beginning of cloud-to-ground and low-altitude intracloud flashes. Such breakdown is the downward analog of upward negative breakdown at the beginning of normal-polarity intracloud discharges, increasingly determined to be the primary cause of terrestrial gamma-ray flashes detected by satellites. The present results support the prediction that downward TGFs are similarly produced during the initial breakdown

of the negative cloud-to-ground (–CG) discharges. The observations differ to those reported for other ground-based observations of TGFs, in that they do not occur during upward positive breakdown of triggered flashes, or during the later stages of –CG return strokes. The TGFs observed by the TASD occur in the beginning stage of negative breakdown, which is likely the most fundamental generating process.

Direct measurement of the photon energy spectrum of the TASD trigger burst showers is not possible with thin scintillator detectors. However, much about the nature of the showers can be inferred from the fact that the showers passed through substantial atmosphere of 1 km or more, and several millimeters of surface detector steel before depositing energy in the scintillator. Note that gamma showers with energies above 100 keV have an attenuation length of order 100 meters at the elevation of the TA detector. To investigate this, we performed a series of Geant4 [*Agostinelli et al.*, 2003; *Allison et al.*, 2006] simulations in order to model the propagation through the atmosphere and the expected TASD response to downward-directed photon showers with primary energies between 100 keV and 100 MeV. (We find that no detectable energy is deposited in the TASD scintillator by primary photons with energy of less than 100 keV starting at altitudes greater than one kilometer above ground level.) Photons were generated according to a RREA spectrum

$$\frac{dN}{dE} \sim \frac{e^{-E/(7\text{MeV})}}{E} \tag{1}$$

where E is the photon energy above 10 keV [*Xu*, 2015]. Based on our observation of the shower footprint size and leader altitudes, particles are assumed to be forward beamed within a cone of half-angle 16°. The angular distribution is assumed to be isotropic within that cone. Particles are then tracked through the atmosphere and a model of the TASD as described in Section 2.1. The TASD-observed maximum VEM (Table S1) are consistent with showers consisting of approximately 10^{14} primary photons at an altitude of several kilometers as shown in Fig. 1.

5 Conclusion

Taken together, the ground level observations presented here satisfy the general description of downward-directed Terrestrial Gamma Flashes associated with downward negative lightning leaders. The key points include:

- Bursts of radiation commencing in the first 1–2 ms of leader formation.
- Burst duration of order several hundred microseconds.

- The footprint on the ground of shower particles associated with the bursts are typically ~ 3-5 km in size.
- The shower source altitudes are typically several kilometers above ground.
- Simulation studies indicate a threshold for detection of above 100 keV for photons created at these altitudes.
- Simulation studies indicating an energy deposit consistent with showers consisting of 10^{14} or more primary photons following a RREA spectrum.

Currently, both the LMA network and slow antenna electric field change instrument remain deployed at the Telescope Array site. An expansion by a factor of four in the coverage area of TASD is planned within the next several years. A plan is in place to deploy additional slow as well as fast electric field sensors covering the expanded TASD detector. This will enable us to study the relation between SD observations and the development of negative breakdown in greater detail. Combined with prolonged operation periods and continuous TA, LMA, and electric field observations, future studies will enable us to better identify and constrain the mechanisms of TGF production.

6 Acknowledgements

References

Abu-Zayyad, T., et al. (2013a), The surface detector array of the Telescope Array experiment, *Nucl. Instrum. Meth.*, *A689*, 87–97, doi:10.1016/j.nima.2012.05.079.

Abu-Zayyad, T., et al. (2013b), The Cosmic Ray Energy Spectrum Observed with the Surface Detector of the Telescope Array Experiment, *Astrophys. J.*, *768*, L1, doi:10.1088/2041-8205/768/1/L1.

Agostinelli, S., et al. (2003), GEANT4: A Simulation toolkit, *Nucl. Instrum. Meth.*, *A506*, 250–303, doi:10.1016/S0168-9002(03)01368-8.

Allison, J., et al. (2006), Geant4 developments and applications, *IEEE Trans. Nucl. Sci.*, *53*, 270, doi:10.1109/TNS.2006.869826.

Behnke, S. A., et al. (2005), Initial leader velocities during intracloud lightning: Possible evidence for a runaway breakdown effect, *J. Geophys. Res.*, *110*, D10,207.

Cummer, S. A., et al. (2011), The lightning-tgf relationship on microsecond timescales, *Geophys. Res. Lett.*, *38*, L14,810, doi:10.1029/2011GL048099.

Cummer, S. A., et al. (2015), Lightning leader altitude progression in terrestrial gamma-ray flashes, *Geophys. Res. Lett.*, *42*, 7792âĂŞ7798, doi:10.1002/2015GL065228.

Dwyer, et al. (2004), A ground level gamma-ray burst observed in association with rocket-triggered lightning, *Geophysical Research Letters*, *31*(5), n/a–n/a, doi:10.1029/2003GL018771, l05119.

Dwyer, et al. (2012a), Observation of a gamma-ray flash at ground level in association with a cloud-to-ground lightning return stroke, *Journal of Geophysical Research: Space Physics*, *117*(A10), n/a–n/a, doi:10.1029/2012JA017810, a10303.

Dwyer, J. R. (2008), The source mechanisms of terrestrial gamma-ray flashes (tgfs), *J. Geophys. Res.*, *113*, D10.

Dwyer, J. R. (2012), The relativistic feedback discharge model of terrestrial gamma ray flashes, *J. Geophys. Res.*, *117*, A02,308, doi:10.1029/2011JA017160.

Dwyer, J. R., and D. M. Smith (2005), A comparison between monte carlo simulations of runaway breakdown and terrestrial gamma-ray flash observations, *Geophysical Research Letters*, *32*(22), doi:10.1029/2005GL023848, l22804.

Dwyer, J. R., et al. (2012b), High energy atmospheric physics: terrestrial gamma-ray flashes and related phenomena, *Space Science Rev.*, *173*, 133–196, doi:10.1007/s11214-012-9894-0.

Fishman, G. J., et al. (1994), Discovery of intense gamma-ray flashes of atmospheric origin, *Science*, *264*, 1313.

Hare, B. M., et al. (2016), Ground-level observation of a terrestrial gamma ray flash initiated by triggered lightning, *J. Geophys. Res.*, *121*, 6511–6533, doi:10.1002/2015JD024426.

Ivanov, D. (2012), Energy Spectrum Measured by the Telescope Array Surface Detector, Ph.D. thesis, University of Utah.

Kouveliotou, C. (1994), BATSE results on observational properties of gamma-ray bursts, *The Astrophysical Journal Supplement*, *92*, 637–642, doi:10.1086/192032.

Krehbiel, P. R., et al. (1979), An analysis of the charge structure of lightning discharges to ground, *J. Geophys. Res.*, *84*, 2432–2456.

Lu, G., et al. (2010), Lightning mapping observation of a terrestrial gamma ray flash, *Geophys. Res. Lett.*, *37*, L11,806, doi:10.1029/2010GL043494.

Lyu, F., et al. (2016), Ground detection of terrestrial gamma ray flashes from distant radio signals, *Geophys. Res. Lett.*, *43*, n/a–n/a, doi:10.1088/2041-8205/768/1/L1.

Nonaka, T., et al. (2009), Performance of the Surface Detector of the Telescope Array experiment, in *Proceedings, 32nd International Cosmic Ray Conference (ICRC 2011): Beijing, China, August 11-18, 2011*, vol. 2, p. 170, doi:10.7529/ICRC2011/V02/0984.

Okuda, T. (2016), Burst Shower Events Observed by the Telescope Array Surface Detector, *PoS*, *ICRC2015*, 298.

Rison, W., et al. (1999), A gps-based three-dimensional lightning mapping system: Initial observations in central new mexico, *Geophysical Research Letters*, *26*(23), 3573–3576.

Rison, W., et al. (2016), Observations of narrow bipolar events reveal how lightning is initiated in thunderstorms, *Nat. Commun.*, *7*, 10,721, doi:10.1038/ncomms10721.

Shao, X., et al. (2010), A closer examination of terrestrial gamma ray flash related lightning processes, *J. Geophys. Res.*, *115*, A00E30, doi:10.1029/2009JA014835.

Shao, X. M., and P. R. Krehbiel (1996), The spatial and temporal development of intracloud lightning, *J. Geophys. Res.*, *101*, 26,641âĂŞ26,668.

Stanley, et al. (2006), A link between terrestrial gamma-ray flashes and intracloud lightning discharges, *Geophysical Research Letters*, *33*(6), n/a–n/a, doi:10.1029/2005GL025537, l06803.

Thomas, R. J., , et al. (2004), Accuracy of the lightning mapping array, *Journal of Geophysical Research: Atmospheres*, *109*(D14), n/a–n/a, d14207.

Thomas, R. J., et al. (2001), Observations of vhf source powers radiated by lightning, *Geophys. Res. Lett.*, *28*, 143–146.

Tran, M., et al. (2015), A terrestrial gamma-ray flash recorded at the lightning observatory in gainesville, florida, *Journal of Atmospheric and Solar-Terrestrial Physics*, *136, Part A*, 86 – 93, advances in Lightning Research.

Xu, W. (2015), Monte Carlo Simulation of Terrestrial Gamma-Ray Flashes Produced by Stepping Lightning Leaders, Ph.D. thesis, The Pennsylvania State University.